



University
of Glasgow

Beniwal, A. , Neethipathi, D. K. and Dahiya, R. (2023) PEDOT:PSS coated screen printed graphene-carbon ink based humidity and temperature sensor. *IEEE Journal on Flexible Electronics*, 2(2), pp. 111-118. (doi: [10.1109/JFLEX.2022.3228970](https://doi.org/10.1109/JFLEX.2022.3228970))

Copyright © 2023, IEEE.

Reproduced under a Creative Commons License.

<https://creativecommons.org/licenses/by/4.0/>

<https://eprints.gla.ac.uk/288300/>

Deposited on: 21 December 2022

Enlighten – Research publications by members of the University of Glasgow
<https://eprints.gla.ac.uk>

PEDOT:PSS coated Screen Printed Graphene-Carbon Ink based Humidity and Temperature Sensor

Ajay Beniwal, Deepan Kumar Neethipathi, Ravinder Dahiya* *Fellow, IEEE*

Abstract— This work presents a multifunctional humidity and temperature sensor, fabricated on a flexible polyvinyl chloride (PVC) substrate using a facile screen-printing and drop casting. The sensor comprises of screen-printed graphene-carbon (G-C) layer coated with Poly(3,4-ethylenedioxythiophene):polystyrene sulfonate (PEDOT:PSS). The sensor displays good sensing performance ($\sim 1\%/ \%RH$) towards wide humidity range (25 %RH - 90 %RH) at room temperature (RT; $27\text{ }^\circ\text{C} \pm 2\text{ }^\circ\text{C}$). The influence of operating temperature on humidity sensing performance is examined in the temperature range of 15 - 55 $^\circ\text{C}$ and a nearly linear relation (with Adj. R^2 of value 0.959) is observed towards change in temperature (35 to 55 $^\circ\text{C}$). Further, temperature sensing performance of the sensor is analysed in 15 - 35 $^\circ\text{C}$ temperature range. The sensor displays good performance with temperature coefficient of resistance as $-3.18\text{ } \%/^\circ\text{C}^{-1}$ and $-1.3\text{ } \%/^\circ\text{C}^{-1}$ for 15-25 $^\circ\text{C}$ and 25-35 $^\circ\text{C}$, respectively. Other important sensing characteristics like repeatability, hysteresis, response, and recovery times are also analysed and presented here.

Index Terms— Flexible sensor, humidity, multifunctional sensor, PEDOT:PSS, printed electronics, temperature.

I. INTRODUCTION

HUMIDITY and temperature sensing is of significant interest in applications such as environment monitoring [1], personal healthcare [2-5], electronic skin (e-Skin) [6-8], food packaging [9-11], and agriculture [12, 13] etc. The regular and continuous monitoring of these parameters is important in above applications. For example, most of greenhouse plants/crops require relative humidity in/around the range of 40 - 80% [14-16] and optimal air temperatures in/around 17 - 27 $^\circ\text{C}$ range [13, 15, 17]. This means it is important to maintain the desired levels of humidity and temperature to ensure high growth rates of greenhouse crops/plants. This need for humidity and temperature measurements calls for cost-effective sensors and as a result wide variety (e.g., capacitive, resistive) of temperature and humidity sensors have been explored [6, 7, 18-23]. However, complex synthesis, non-flexible form factors and cost-

ineffective fabrication hinder their widespread use. In this regard, printed sensors on flexible substrates offer an attractive route for flexible electronics applications [24-26]. The capability to choose the printing ink, substrate, and the flexibility of designing the electrode with desired pattern offers numerous opportunities to enhance the performance of these sensors. Further, the resource efficient printing could improve the commercial viability of these sensors [27].

Among various sensitive materials, the inks based on carbon and graphite have been explored extensively for chemical, physical and biosensors [28-30]. Similarly, conductive polymers such as PEDOT:PSS have been extensively reported for numerous sensing applications [6, 31, 32]. The key features of PEDOT:PSS which makes it suitable for sensors are its tunable conductivity, good thermal stability, good transparency to visible light, compatibility towards solution-based processes and a high level of biocompatibility [33]. Whilst several PEDOT:PSS based humidity [20, 31, 34-38] and temperature [2, 4, 6, 39-41] sensors have been reported. However, the use of metal-based inks for electrodes, limited sensing performance, complex fabrication route and singular function of the sensor adds to another layer of complication. Therefore, the ease of fabrication from these materials is still a challenge specifically for developing a multifunctional sensor (e.g., temperature and humidity) which has advantages such as low power consumption, compact structure, reduced cost, and small size [3, 42, 43].

Herein, we report a simple strategy for development of a multifunctional sensor (for humidity and temperature sensing) involving the drop casting of PEDOT:PSS over a graphene-carbon screen-printed layer/electrode. The PEDOT:PSS/G-C ink based flexible, multifunctional sensor's performance is investigated towards humidity and temperature sensing in range 25-90 %RH and 15-35 $^\circ\text{C}$, respectively. The detailed study about the influence of temperature on humidity sensing also provides insight into using the developed sensor for humidity monitoring under different operating temperatures. The printing of biocompatible G-C ink for electrodes is resource efficient methods as compared to conventional metal deposition

This work was supported in part by the Engineering and Physical Sciences Research Council through Engineering Fellowship for Growth (EP/R029644/1) and European Commission through Innovative Training Network AQUASENSE (H2020-MSCA-ITN-2018-813680). (*Corresponding author: Ravinder Dahiya*).

A. Beniwal and D. K. Neethipathi are with James Watt School of Engineering, University of Glasgow, Glasgow G12 8QQ, U.K.

R. Dahiya is with Bendable Electronics and Sustainable Technologies (BEST) Group, ECE Department, Northeastern University, Boston, MA 02115, USA. The work in this paper was initiated by R. Dahiya's Bendable Electronics and Sensing Technologies (BEST) Group when he was at University of Glasgow, UK. The work got completed after he moved to Northeastern University, USA, where his group is known as Bendable Electronics and Sustainable Technologies (BEST) Group (email – r.dahiya@northeastern.edu)

An earlier version of this paper was presented at 2022 IEEE International Conference on Flexible and Printable Sensors and Systems (FLEPS) (DOI: 10.1109/FLEPS53764.2022.9781534).

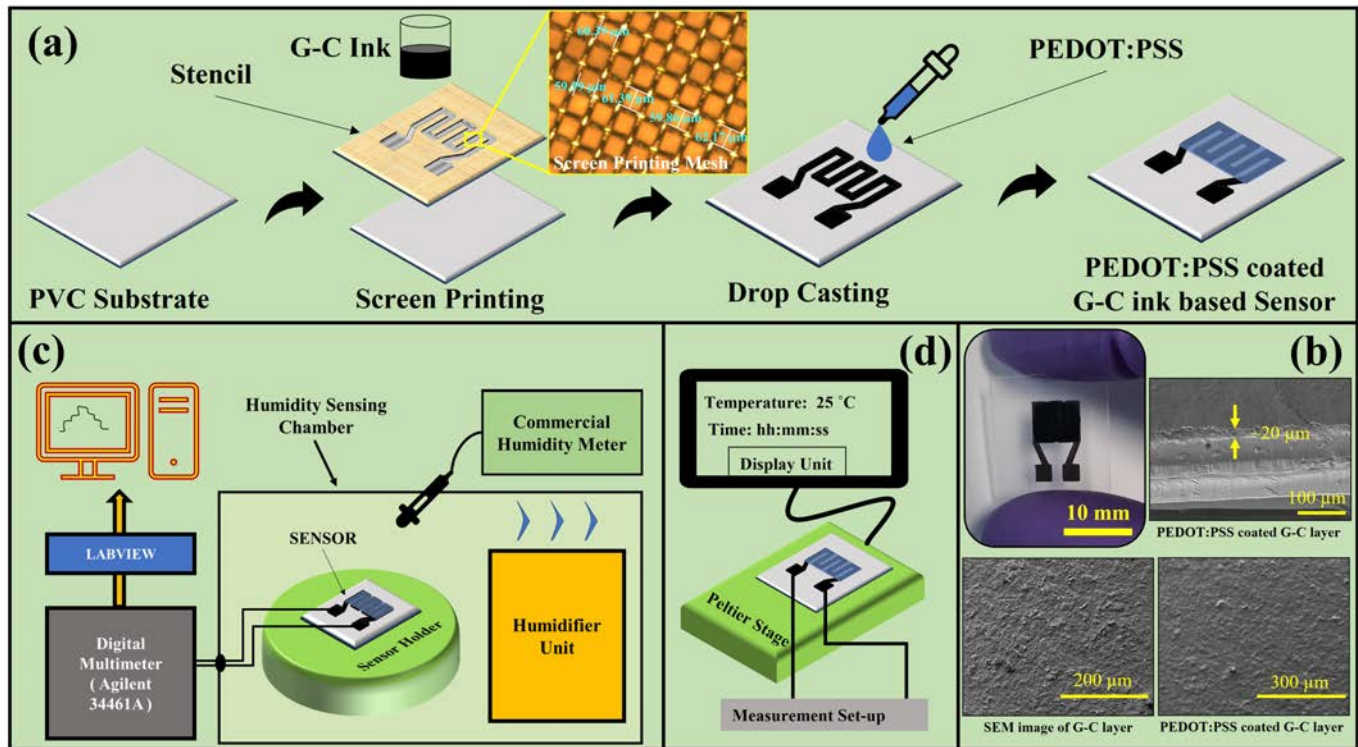


Fig. 1. (a) Schematic illustration of the fabrication process for PEDOT:PSS coated G-C ink based multifunctional sensor. (b) Fabricated sensor and SEM images of the G-C layer and PEDOT:PSS coated G-C sensing layer. Schematic illustration of the (c) humidity sensing set-up and (d) temperature sensing set-up.

methods. The work presented in this paper extends our preliminary results presented at IEEE International Conference on Flexible and Printable Sensors and Systems (FLEPS) 2022 [44]. Here, we have discussed the influence of the operating temperature on humidity sensing characteristics of PEDOT:PSS coated/modified G-C ink-based sensor. Also, the temperature sensing characteristics are analysed by introducing the multifunctionality aspect of the developed sensor.

This paper is organised as follows: The materials and methods used for the development of sensor are given in Section II. The results from evaluation of humidity sensor, temperature sensor and influence of operating temperature on humidity sensing performance are given in Section III and the key outcomes are explained in Section IV.

II. MATERIALS AND METHODS

A. Materials

The flexible polyvinyl chloride (PVC) sheet having $\sim 175 \mu\text{m}$ thickness was used as flexible substrate. PEDOT:PSS used in this work was purchased from Ossila (PEDOT:PSS (PH 1000)). The graphene carbon ink for screen printing the G-C layer was from Sun Chemical (C2171023D1: Graphene Carbon Ink:BG04). Silver conductive (RS 186-3600, RS Components) was used for wire connections/contacts. For wire insulation, the grey dielectric ink (D2070423P5: Grey Dielectric Ink:BG04, Sun Chemical) was used.

B. Fabrication of sensor

The multifunctional humidity and temperature sensor, shown in Fig. 1, was developed using a two-step fabrication process, i.e., screen printing and drop casting. Firstly, screen printer

(Screen Stencil Printer C920, Aurel Automation) was used to print the graphene-carbon ink-based layer on a flexible PVC substrate. The printed layers were annealed for an hour in an oven at 60°C . The wire connections were realised using silver conductive paste for 2-wire resistance measurements and the contacts were insulated using the grey dielectric ink, which was cured in the oven at 60°C for half an hour. After this, screen printed graphene carbon layer was modified by drop casting $30 \mu\text{L}$ of PEDOT:PSS on it. The modified layer was left to dry at 40°C overnight to develop PEDOT:PSS coated graphene-carbon ink based multifunctional sensor (also referred as sensor2). Here, the unmodified i.e., graphene-carbon ink-based sensor is referred as sensor1. The schematic illustration of sensor fabrication steps and developed sensor are shown in Fig. 1 (a-b). The scanning electron microscopy (SEM) images of the G-C layer and PEDOT:PSS coated G-C layer are shown in Fig. 1 (b). The layer thickness of PEDOT:PSS coated G-C ink-based sensing layer is found to be $\sim 20 \mu\text{m}$.

C. Humidity and temperature sensing set-up

For humidity sensing, an acrylic sensing chamber (dimensions: $50 \text{ cm} \times 40 \text{ cm} \times 45 \text{ cm}$) is used. This chamber contains a sensor holder and humidifier unit, placed inside the chamber. A rubber seal is used to cover the top panel airtight. The holes on the sides of panels are used to insert (i) sensor cable for measurement, (ii) commercial humidity meter tip used for calibration purpose, and (iii) a power cord for the humidifier unit. Here PureMate (PM 908 Digital Ultrasonic Cool Mist Humidifier) is utilized as the humidifier unit, which can be used for generating as well as regulating the humidity condition within the chamber. For the calibration, commercially available ATP - Humidity & Temperature Meter DT-625 is used as the

> REPLACE THIS LINE WITH YOUR MANUSCRIPT ID NUMBER (DOUBLE-CLICK HERE TO EDIT) <

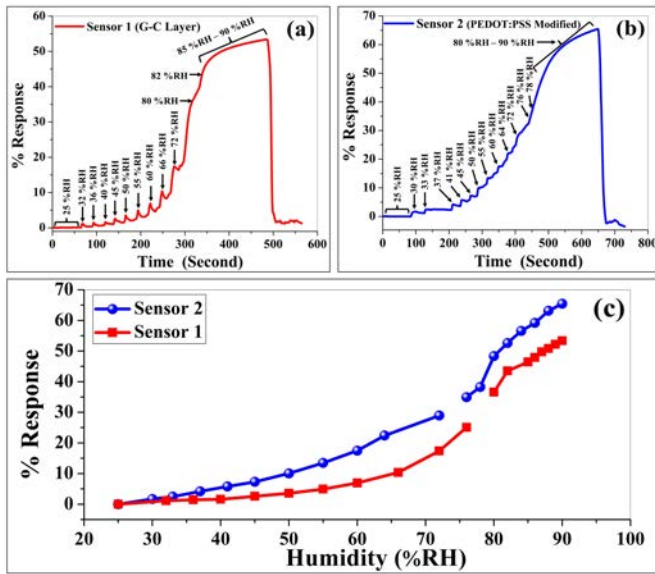


Fig. 2. Humidity sensing characteristics of sensor1 and sensor2 for 25 %RH to 90 %RH range. Dynamic response characteristics of (a) sensor1 and (b) sensor2. (c) % Response for sensor1 and sensor2. [44]

reference humidity meter (with $\pm 2\%$ RH accuracy) and temperature meter. The measurements are carried out using Agilent 34461A 6½ Digit Multimeter and the change in resistance was observed and recorded using the associated LabVIEW interface. For dehumidification process, the top panel of the sensing chamber was set open, and sensor was exposed to air. Further, a Peltier stage (*PE120 Peltier system, Linkam Scientific Instruments Ltd.*) is used to examine the influence of operating temperature on humidity sensing characteristics analysis and temperature sensing characteristics of the developed sensor. The Peltier stage is operated to achieve the desired temperatures. The change in resistance of the sensor is measured using the digital multimeter. The schematic illustrations of humidity and temperature sensing set-ups are shown in Fig. 1 (c-d).

III. RESULTS AND DISCUSSION

A. Humidity sensing analysis

The humidity sensing characteristics for both sensor types i.e., sensor1 (pre-modification G-C layer) and sensor2 (PEDOT:PSS coated/modified G-C layer) was observed in 25 - 90 %RH humidity range at room temperature ($27\text{ }^\circ\text{C} \pm 2\text{ }^\circ\text{C}$) and the results are shown in Fig. 2 (a-b) [44]. The humidity sensing performance is examined using % response, which is determined as follows [45]:

$$\frac{\Delta R}{R_A} \times 100 \quad (1)$$

Where, $\Delta R = R_H - R_A$; R_H is resistance of the sensor defined at particular humidity level and R_A is the baseline resistance (analysed at 25 %RH). The comparative analysis of humidity sensing performance, displayed in Fig. 2(c) [44], clearly shows the enhanced performance of sensor2 as compared to sensor1, specifically for low to moderate humidity range (below and around 60 %RH). The reproducibility analysis was also carried out for sensor2 by repeating the fabrication route and developing replica sensors (RS). The responses of the replica sensors i.e.,

RS (i), RS (ii) and RS3 (iii) are compared with the original sensor2 (referred as humidity sensor) in the Fig. 3 (a-d). The obtained responses of the replica sensors are found well in accordance with the original humidity sensor with minor variations in % response.

Therefore, the obtained results suggest possible applicability of sensor2 towards various humidity sensing applications. For example, the obtained sensing performance ($\sim 1\text{ } \%/ \%$ RH) in the range 25-90 %RH indicates the suitability of the sensor for potential greenhouse application. Considering the enhanced humidity sensing performance of sensor2, further characterisations (e.g., influence of temperature on humidity sensing performance, multifunctionality analysis with temperature sensing measurement etc.) were examined using PEDOT: PSS coated G-C layer-based sensor i.e., sensor2. Hence, hereafter sensor2 is referred as the humidity and/or temperature or multifunctional sensor, unless otherwise stated.

B. Influence of operating temperature on humidity sensing performance sensor

Along with the humidity, the change in temperature also affects the electrical properties of PEDOT:PSS [46]. Therefore, it is important to understand the influence of temperature variations on humidity sensing, specifically for applications where monitoring of both the parameters i.e., humidity as well as temperature is important (e.g., greenhouse industries). The temperature sensing properties of pristine or functionalized PEDOT:PSS are well reported in the literature [2, 4, 6, 39]. Nonetheless, the influence of the temperature variations on humidity sensing properties of PEDOT:PSS based sensor is important and hence, examined in the present work. The performance of the developed humidity sensor (replica sensor) was examined in a temperature range of 15 - 55 °C and humidity range of 25 - 90 %RH, as shown in the Fig. 4. Initially, the performance of the sensor was evaluated at room temperature (25 °C). Further, it was analysed by considering temperature variation in both the directions i.e., increase and decrease with respect to RT. The change in resistance for considered humidity range is depicted in Fig. 4 (a) in terms of % responses at 15, 25, 35, 45 and 55 °C. The observed % responses, shown in the Fig.

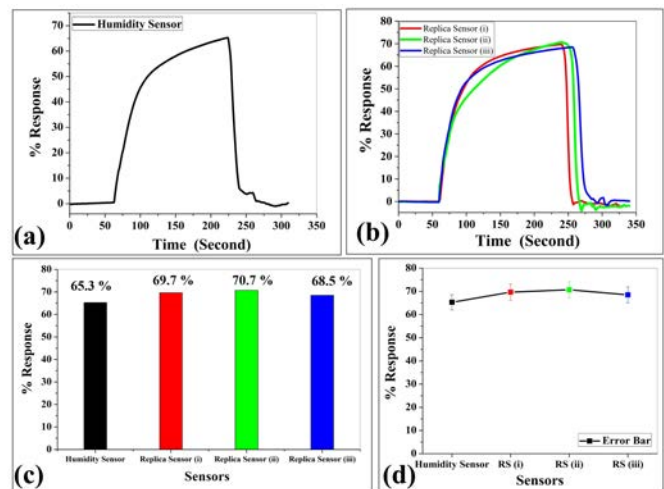


Fig. 3. Reproducibility analysis of (a) original humidity sensor and (b) replica sensors for 25 %RH to 90 %RH range. (c) Comparative analysis of % responses of replica sensor with original sensor. (d) Error bar for original and three replica sensors.

> REPLACE THIS LINE WITH YOUR MANUSCRIPT ID NUMBER (DOUBLE-CLICK HERE TO EDIT) <

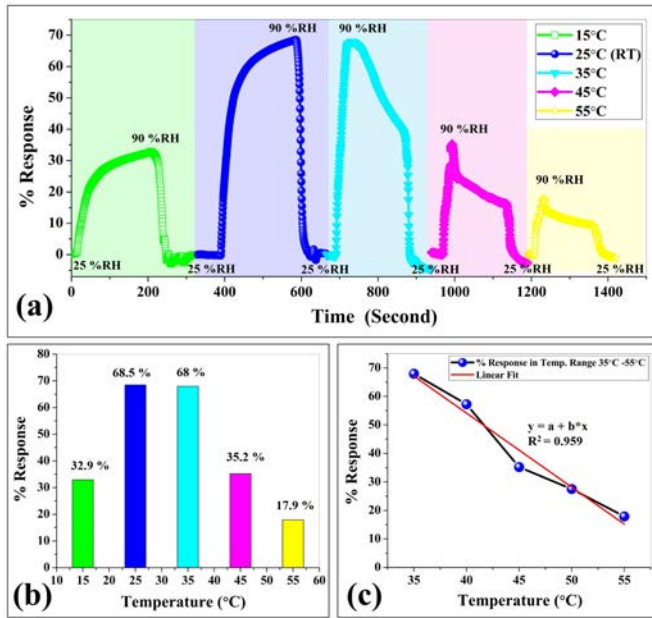


Fig. 4. Influence of operating temperature on humidity sensing performance of PEDOT:PSS modified sensor. (a) Humidity sensing characteristics analysis for temperature range 15 - 55 °C towards 25 %RH to 90 %RH. The % response analysis (for humidity sensing) in temperature range (b) 15 - 55 °C at an interval of 10 °C and (c) 35 - 55 °C at an interval of 5 °C.

4 (b), are 32.9%, 68.5%, 68%, 35.2% and 17.9% at 15, 25, 35, 45 and 55 °C, respectively, for considered humidity range i.e., 25 - 90 %RH. The obtained results indicate that humidity sensing performance is significantly influenced by the operating temperature conditions and the influence can be seen in both the directions of temperature variation. This could be explained via humidity sensing mechanism at RT and other temperatures. At RT, under humid conditions the sensing layer absorb moisture/water and hydrophilic PSS may swell. The latter leads to larger distances between adjacent PEDOT enriched cores, which increases the resistance of the sensing layer. However, under elevated temperature conditions, the moisture will be desorbed from the sensing layer. This will reduce the total number and the size of particle boundaries (these boundaries prevent charge carrier hopping between PEDOT:PSS) and thus, lead to decrease in resistance of the sensing layer [33, 39]. Further, the humidity sensing performance for 5 °C temperature variation in 35 - 55 °C range is also analysed and shown in the Fig. 4 (c). The calculated humidity sensing % response is found to be decreasing (68% to 17.9%) towards this change in operating temperature conditions (35 - 55 °C). The observed value (0.959) of the coefficient of linearity (R^2), demonstrates nearly linear declining % response for humidity sensing in the operating temperature conditions (35 - 55 °C). Therefore, by applying the suitable mathematical modelling or temperature compensation model the developed sensor could be used in a wide operating temperature condition. However, further experiments and data are needed to develop this model. Therefore, the observed influence of operating temperature conditions on humidity sensing characteristics (interestingly, a nearly linear relationship is observed) signify that the developed sensor has the potential to be used as a multifunctional sensor capable of monitoring humidity as well as temperature. Multifunctionality of most of the sensors focus on two sensing capabilities, under relatively stable behaviour of one signal, sensor detect another signal effectively, and vice versa [42]. The

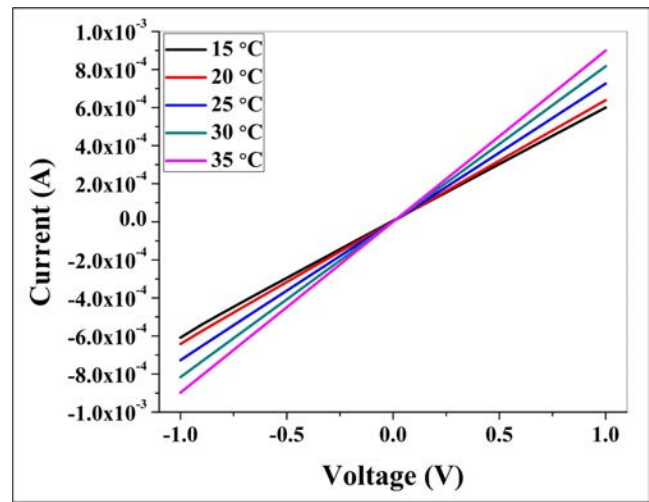


Fig. 5. Temperature dependent I-V characteristics of the sensor with a voltage sweep from -1 V to +1 V in temperature range 15 - 35 °C.

multifunctional sensor also offers several advantages like low power consumption, compact structure, reduced cost, and small size [3, 42, 43].

The results obtained from the influence of operating temperature on humidity sensing performance indicate the suitability of the sensor towards temperature sensing applications also. Therefore, a systematic study was carried out to understand the temperature sensing properties of the PEDOT:PSS based multifunction sensor. The temperature sensing characteristics have been analysed in detail considering the suitability of the developed multifunction sensor for potential application i.e., greenhouse industries.

C. Temperature sensing performance analysis

The temperature sensing response of the developed sensor was analysed in 15 - 35 °C range. This temperature range is

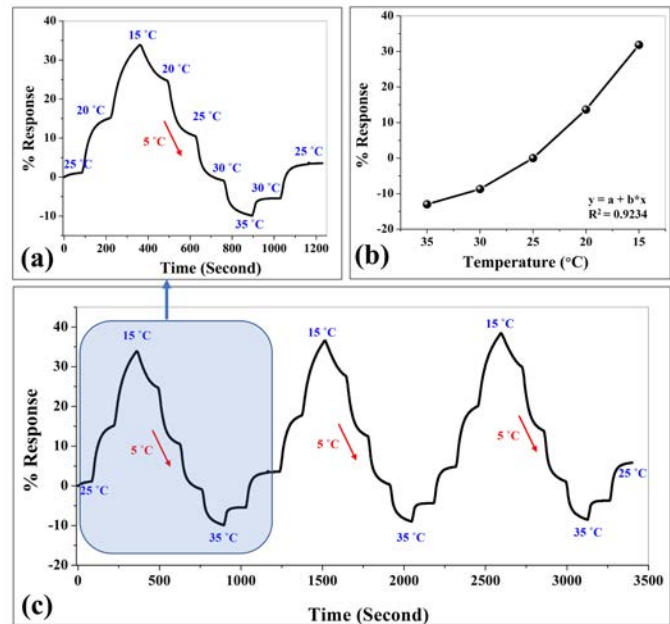


Fig. 6. Temperature sensing performance analysis (a) stepwise response of the sensor in temperature range 15 °C - 35 °C with a step change of 5 °C. (b) % Response vs temperature graph. (c) Three-cyclic repeatability analysis of the sensor in temperature range 15 °C - 35 °C with a step change profile of 5 °C.

> REPLACE THIS LINE WITH YOUR MANUSCRIPT ID NUMBER (DOUBLE-CLICK HERE TO EDIT) <

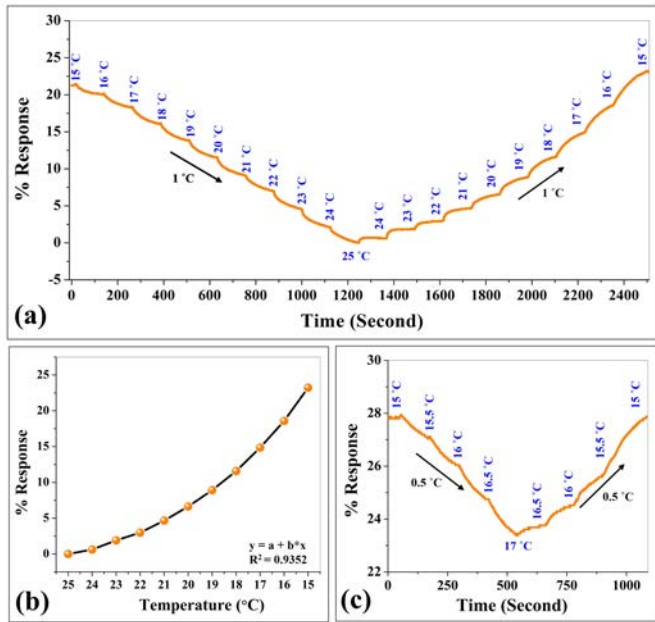


Fig. 7. Temperature sensing performance analysis (a) stepwise response of the sensor in temperature range 15 °C - 25 °C with a step change of 1 °C. (b) % Response vs temperature graph. (c) Stepwise response of the sensor in temperature range 15 °C - 17 °C with a step change of 0.5 °C.

considered based on the requirement of the proposed multifunction sensor for potential application (greenhouse industries). The optimal air temperatures for greenhouse crops is reported in/around the range of 17 – 27 °C [13]. Initially, the I-V characteristics of the sensor were obtained with a voltage sweep from -1 V to +1 V in temperature range 15 - 35 °C as displayed in Fig. 5. The increase in current with temperature indicates the enhanced conductivity with increase in temperature. The stepwise (step change of 5 °C) response of the sensor in temperature range 15 - 35 °C is shown in Fig. 6 (a). The resistance of the sensor observed at RT is considered as baseline resistance used for calculations of % response. The % response is analysed using the formula given in Eq. 2.

$$\frac{\Delta R}{R_A} \times 100 \quad (2)$$

For temperature sensing, $\Delta R = R_T - R_A$; R_T is resistance of the sensor at a particular temperature and R_A is the baseline resistance (analysed at room temperature i.e., 25 °C). The % response vs temperature graph is shown in Fig. 6 (b). The calculated % responses are found to be in positive to negative range (~ +32 % to ~ -13 %) based on the change in resistance behaviour (with respect to baseline resistance) of the sensor towards the temperature sensing (15 - 35 °C). The coefficient of linearity (R^2) is observed as 0.9234. Furthermore, the temperature coefficient of resistance (TCR) is obtained from the data displayed in Fig. 6. The TCR (α) is determined as follows [39, 47]:

$$R = R_{Ref} [1 + \alpha(T - T_{Ref})] \quad (3)$$

Where, R_{Ref} and T_{Ref} are considered as resistance and temperature, respectively, at RT (25 °C) conditions. TCR was observed separately for 15-25 °C (TCR1) and 25-35 °C (TCR2). The calculated TCR1 and TCR2 are found to be -3.18 %°C⁻¹ and -1.3 %°C⁻¹, respectively. The obtained negative TCR of the developed PEDOT:PSS/G-C ink-based sensor is well supported by the background studies [6, 33, 39] and could be explained as

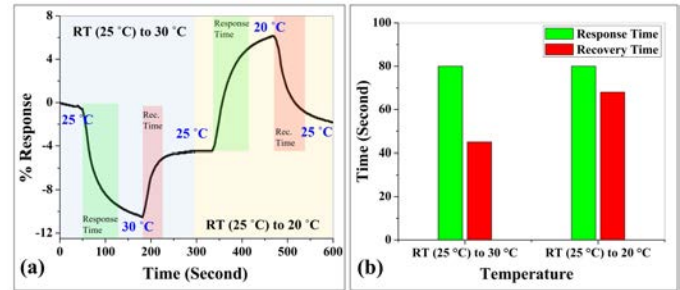


Fig. 8. (a) Response and recovery time analysis of the sensor for RT (25 °C) - 30 °C and RT (25 °C) - 20 °C. (b) Comparative analysis of response and recovery time for RT (25 °C) - 30 °C and RT (25 °C) - 20 °C.

follows: PEDOT:PSS exhibits a core-shell grain like structure having hydrophobic and conductive PEDOT-rich core surrounded by hydrophilic and insulating PSS-rich shell [33]. With increase in temperature, generation and enhancement of charge carriers transport in PEDOT:PSS based sensor triggers the decrease in the resistance of the sensing layer. Also, increased thermal energy (with temperature) causes enhancement in limited carrier tunneling and hopping within individual as well as neighbored grains [39, 48]. Therefore, resistance of the sensor decreases with increase in temperature i.e., negative temperature coefficient.

The repeatability analysis of the sensor was also performed by measuring response in three-cyclic temperatures in 15 - 35 °C range, again with a step of 5 °C. The obtained results, as shown in the Fig. 6 (c), indicate good repeatability of the sensor towards temperature sensing. Moreover, to define the resolution of the sensor towards temperature sensing characteristics, the sensing is also analysed with a step change of 1 °C and 0.5 °C. The observed stepwise response of the sensor in temperature range 15 - 25 °C with a step change of 1 °C (as shown in Fig. 7 (a-b)) and 0.5 °C (as displayed in Fig. 7 (c)) indicates the sensor is also suitable for detection of small temperature variations.

Finally, the response-recovery times and hysteresis were also measured. The response and recovery times analysed for both increase and decrease in temperature (from RT) are shown in Fig. 8. The response/recovery times for RT (25 °C) - 30 °C are

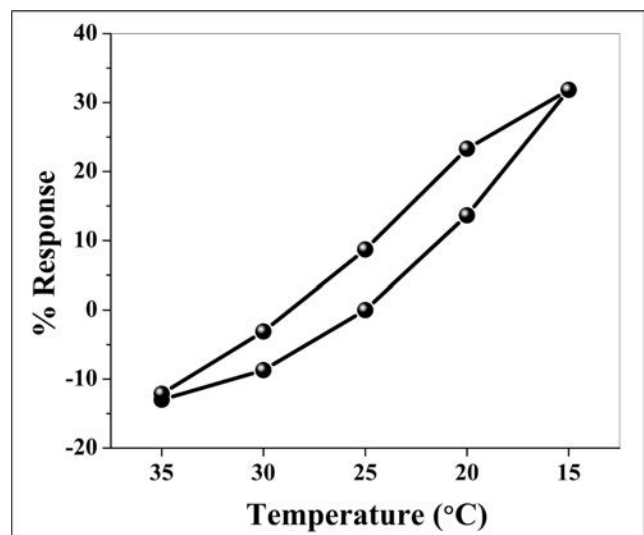


Fig. 9. Hysteresis profile of the sensor with stepwise response of the sensor in temperature range 15 °C - 35 °C.

> REPLACE THIS LINE WITH YOUR MANUSCRIPT ID NUMBER (DOUBLE-CLICK HERE TO EDIT) <

observed as ~80s/45s and for RT (25 °C) - 20 °C found to be ~80s/68s. The hysteresis profile of the sensor is shown in Fig. 9. The results indicates that sensor exhibits some hysteresis towards temperature sensing in considered range which could be ascribed to the multifunctionality of the sensor i.e., sensitivity towards humidity as well. Therefore, further studies need to be performed by encapsulating the sensing layer and analysing the impact of encapsulation on sensing performance.

IV. CONCLUSION

In this work, a PEDOT:PSS coated graphene-carbon ink based flexible and multifunctional (humidity and temperature) sensor has been presented. A simple, and cost-effective screen-printed technique followed by drop casting method is used for sensor fabrication. The sensor displays good response (~1 %/%RH) and reproducible sensing performance over a wide humidity range (25 %RH - 90 %RH) at room temperature (RT; 27 °C ± 2 °C). The influence of operating temperature conditions on humidity measurements signifies the potential of developed sensor for multifunctional sensing. A nearly linear relationship (with Adj. R² of value 0.959) is observed with declining % response (~68% to ~18%) for humidity sensing towards change in temperature (35 - 55 °C). Obtained results indicate that a mathematical compensation model could be applied to use the sensor suitable for wide/fluctuating operating temperature conditions. However, further experiments and data are needed to develop such a model. Further, the temperature sensing performance of the sensor has been analysed in temperature range 15 - 35 °C and sensor exhibits good performance with TCRs of -3.18 %°C⁻¹ and -1.3 %°C⁻¹ for 15 - 25 °C and 25 - 35 °C, respectively. Other sensing characteristics such as repeatability (3-cyclic), hysteresis (15 - 35 °C), the response and recovery times (~80s and ~45s for 25 - 30°C) etc. are also obtained. The results indicate the suitability of the developed multifunctional sensor for potential application in greenhouse industry and various other sectors such as environmental monitoring, industrial, agriculture and healthcare applications.

REFERENCES

- [1] R. Malik, V. K. Tomer, V. Chaudhary, M. S. Dahiya, A. Sharma, S. Nehra, S. Duhan, and K. Kailasam, "An excellent humidity sensor based on In-SnO₂ loaded mesoporous graphitic carbon nitride," *Journal of Materials Chemistry A*, vol. 5, no. 27, pp. 14134-14143, 2017.
- [2] Y. Yu, S. Peng, P. Blanloeuil, S. Wu, and C. H. Wang, "Wearable Temperature Sensors with Enhanced Sensitivity by Engineering Microcrack Morphology in PEDOT:PSS-PDMS Sensors," *ACS Applied Materials & Interfaces*, vol. 12, no. 32, pp. 36578-36588, 2020.
- [3] J. Wu, Z. Wu, H. Ding, Y. Wei, X. Yang, Z. Li, B.-R. Yang, C. Liu, L. Qiu, and X. Wang, "Multifunctional and High-Sensitive Sensor Capable of Detecting Humidity, Temperature, and Flow Stimuli Using an Integrated Microheater," *ACS Applied Materials & Interfaces*, vol. 11, no. 46, pp. 43383-43392, 2019.
- [4] B. A. Kuzubasoglu, E. Sayar, and S. K. Bahadir, "Inkjet-Printed CNT/PEDOT:PSS Temperature Sensor on a Textile Substrate for Wearable Intelligent Systems," *IEEE Sensors J.*, vol. 21, no. 12, pp. 13090-13097, 2021.
- [5] Y. Wang, L. Zhang, Z. Zhang, P. Sun, and H. Chen, "High-sensitivity wearable and flexible humidity sensor based on graphene oxide/non-woven fabric for respiration monitoring," *Langmuir*, vol. 36, no. 32, pp. 9443-9448, 2020.
- [6] M. Soni, M. Bhattacharjee, M. Ntagios, and R. Dahiya, "Printed Temperature Sensor Based on PEDOT: PSS-Graphene Oxide Composite," *IEEE Sensors J.*, vol. 20, no. 14, pp. 7525-7531, 2020.
- [7] J. Neto, R. Chirila, A. S. Dahiya, A. Christou, D. Shakthivel, and R. Dahiya, "Skin-Inspired Thermoreceptors-Based Electronic Skin for Biomimicking Thermal Pain Reflexes," *Adv. Sc.*, pp. 2201525, 2022, doi: 10.1002/advs.202201525.
- [8] Y. Kumaresan, O. Ozioko, and R. Dahiya, "Multifunctional Electronic Skin With a Stack of Temperature and Pressure Sensor Arrays," *IEEE Sensors J.*, vol. 21, no. 23, pp. 26243-26251, 2021.
- [9] P. Escobedo, M. Bhattacharjee, F. Nikbakhtnasrabadi, and R. Dahiya, "Flexible Strain and Temperature Sensing NFC Tag for Smart Food Packaging Applications," *IEEE Sensors J.* vol. 21, no. 23, pp. 26406-26414, 2021.
- [10] Z. Duan, Y. Jiang, and H. Tai, "Recent advances in humidity sensor for human body related humidity detections," *J. Materials Chemistry C*, vol. 9, pp. 14963-14980, 2021.
- [11] M. Parthibavarman, V. Hariharan, and C. Sekar, "High-sensitivity humidity sensor based on SnO₂ nanoparticles synthesized by microwave irradiation method," *Materials Sc. and Engineering: C*, vol. 31, no. 5, pp. 840-844, 2011.
- [12] F. Romero, S. Cazzato, F. Walder, S. Vogelgsang, S. F. Bender, and M. G. van der Heijden, "Humidity and high temperature are important for predicting fungal disease outbreaks worldwide," *New Phytologist*, vol. 234, pp. 1553-1556, 2022.
- [13] R. R. Shamshiri, J. W. Jones, K. R. Thorp, D. Ahmad, H. C. Man, and S. Taheri, "Review of optimum temperature, humidity, and vapour pressure deficit for microclimate evaluation and control in greenhouse cultivation of tomato: a review," *Int. Agrophysics*, vol. 32, no. 2, pp. 287-302, 2018.
- [14] O. Räsänen, "How Can You Maintain the Ideal Humidity in a Greenhouse?," *Ruuvii Innovations Ltd*, Riihimäki, Finland, 12 Nov., 2021. Available: <https://ruuvii.com/how-can-you-maintain-the-ideal-humidity-in-a-greenhouse/>. [Accessed on: 05 Sept. 2022].
- [15] DryGair, "Greenhouse Humidity And Temperature," *DryGair Energies Ltd.*, Herzliya, Israel. Available: <https://drygair.com/blog/optimal-humidity-temperature-greenhouse/>. [Accessed on: 05 Sept. 2022].
- [16] Y. Hashimoto, T. Morimoto, S. Funada, and J. Sugi, "Optimal Control of Greenhouse Climate by the Identification of Water Deficiency and Photosynthesis in Short-term Plant Growth," *IFAC Proceedings Volumes*, vol. 14, no. 2, pp. 3621-3626, 1981.
- [17] N. Vercelletto, "The ideal greenhouse temperature and humidity settings for every season," *HappySprout*, Portland/New York, USA, 31 Aug., 2022. Available: <https://www.happysprout.com/outdoor-living/greenhouse-temperature-humidity/>. [Accessed on: 05 Sept. 2022].
- [18] S. Dervin, P. Ganguly, and R. Dahiya, "Disposable electrochemical sensor using Graphene oxide-chitosan modified carbon-based electrodes for the detection of tyrosine," *IEEE Sensors J.* vol. 21, no. 23, pp. 26226-26233, 2021.
- [19] M. Bhattacharjee, F. Nikbakhtnasrabadi, and R. Dahiya, "Printed Chipless Antenna as Flexible Temperature Sensor," *IEEE Internet of Things Journal*, vol. 8, no. 6, pp. 5101-5110, 2021.
- [20] X. Yao, and Y. Cui, "A PEDOT:PSS functionalized capacitive sensor for humidity," *Measurement*, vol. 160, pp. 107782, 2020.
- [21] A. Beniwal, P. Ganguly, A. K. Aliyana, G. Khandelwal, and R. Dahiya, "Screen-printed Graphene-carbon Ink based Disposable Humidity Sensor with Wireless Communication," *Sensors and Actuators B: Chemical*, vol. 374, pp. 132731, 2023.
- [22] Y. Pang, J. Jian, T. Tu, Z. Yang, J. Ling, Y. Li, X. Wang, Y. Qiao, H. Tian, and Y. Yang, "Wearable humidity sensor based on porous graphene network for respiration monitoring," *Biosensors and Bioelectronics*, vol. 116, pp. 123-129, 2018.
- [23] A. K. Aliyana, P. Ganguly, A. Beniwal, N. Kumar S K, and R. Dahiya, "Disposable pH sensor on paper using screen-printed graphene-carbon ink modified zinc oxide nanoparticles," *IEEE Sensors J.* 2022, doi: 10.1109/JSEN.2022.3206212.
- [24] V. S. Turkani, D. Maddipatla, B. B. Narakathu, T. S. Saeed, S. O. Obare, B. J. Bazuin, and M. Z. Atashbar, "A highly sensitive printed humidity sensor based on a functionalized MWCNT/HEC composite for flexible electronics application," *Nanoscale Adv.*, vol. 1, no. 6, pp. 2311-2322, 2019.
- [25] X. Zhang, D. Maddipatla, A. K. Bose, S. Hajian, B. B. Narakathu, J. D. Williams, M. F. Mitchell, and M. Z. Atashbar, "Printed Carbon Nanotubes-Based Flexible Resistive Humidity Sensor," *IEEE Sensors J.* vol. 20, no. 21, pp. 12592-12601, 2020.

> REPLACE THIS LINE WITH YOUR MANUSCRIPT ID NUMBER (DOUBLE-CLICK HERE TO EDIT) <

- [26] V. S. Turkani, D. Maddipatla, B. B. Narakathu, B. J. Bazuin, and M. Z. Atashbar, "A carbon nanotube based NTC thermistor using additive print manufacturing processes," *Sensors and Actuators A: Physical*, vol. 279, pp. 1-9, 2018.
- [27] A. Benchirouf, S. Palaniyappan, R. Ramalingame, P. Raghunandan, T. Jagemann, C. Müller, M. Hietschold, and O. Kanoun, "Electrical properties of multi-walled carbon nanotubes/PEDOT: PSS nanocomposites thin films under temperature and humidity effects," *Sensors and Actuators B: Chemical*, vol. 224, pp. 344-350, 2016.
- [28] P. Karipoth, A. Pullanchiyodan, A. Christou, and R. Dahiya, "Graphite-Based Bioinspired Piezoresistive Soft Strain Sensors with Performance Optimized for Low Strain Values," *ACS Applied Materials & Interfaces*, vol. 13, no. 51, pp. 61610-61619 2021.
- [29] M. A. Kafi, A. Paul, A. Vilouras, E. S. Hosseini, and R. S. Dahiya, "Chitosan-graphene oxide-based ultra-thin and flexible sensor for diabetic wound monitoring," *IEEE Sensors J.*, vol. 20, no. 13, pp. 6794-6801, 2019.
- [30] Y. Kumaresan, S. Mishra, O. Ozioko, R. Chirila, and R. Dahiya, "Ultra-High Gauge Factor Strain Sensor with Wide-Range Stretchability," *Adv. Intelligent Syst.*, pp. 2200043, 2022, doi: 10.1002/aisy.202200043.
- [31] G. Hassan, M. Sajid, and C. Choi, "Highly sensitive and full range detectable humidity sensor using PEDOT: PSS, methyl red and graphene oxide materials," *Scientific reports*, vol. 9, no. 1, pp. 1-10, 2019.
- [32] M. Bhattacharjee, M. Soni, P. Escobedo, and R. Dahiya, "PEDOT: PSS microchannel-based highly sensitive stretchable strain sensor," *Advanced Electronic Materials*, vol. 6, no. 8, pp. 2000445, 2020.
- [33] X. Zhang, W. Yang, H. Zhang, M. Xie, and X. Duan, "PEDOT:PSS: From conductive polymers to sensors," *Nanotechnology and Precision Engineering*, vol. 4, no. 4, pp. 045004, 2021.
- [34] M. Kuş, and S. Okur, "Electrical characterization of PEDOT: PSS beyond humidity saturation," *Sensors and Actuators B: Chemical*, vol. 143, no. 1, pp. 177-181, 2009.
- [35] E. Assunção da Silva, C. Duc, N. Redon, and J. I. Wojkiewicz, "Humidity Sensor Based on PEO/PEDOT: PSS Blends for Breath Monitoring," *Macromolecular Materials and Engineering*, vol. 306, no. 12, pp. 2100489, 2021.
- [36] E. Assunção da Silva, C. Duc, N. Redon, and J.-L. Wojkiewicz, "Humidity Sensor Based on PEO/PEDOT:PSS Blends for Breath Monitoring," *Macromolecular Materials and Engineering*, vol. 306, no. 12, pp. 2100489, 2021.
- [37] R. M. Morais, M. d. S. Klem, G. L. Nogueira, T. C. Gomes, and N. Alves, "Low Cost Humidity Sensor Based on PANI/PEDOT:PSS Printed on Paper," *IEEE Sensors J.* vol. 18, no. 7, pp. 2647-2651, 2018.
- [38] S. Taccola, F. Greco, A. Zucca, C. Innocenti, C. de Julián Fernández, G. Campo, C. Sangregorio, B. Mazzolai, and V. Mattoli, "Characterization of Free-Standing PEDOT:PSS/Iron Oxide Nanoparticle Composite Thin Films and Application As Conformable Humidity Sensors," *ACS Applied Materials & Interfaces*, vol. 5, no. 13, pp. 6324-6332, 2013.
- [39] Y.-F. Wang, T. Sekine, Y. Takeda, K. Yokosawa, H. Matsui, D. Kumaki, T. Shiba, T. Nishikawa, and S. Tokito, "Fully Printed PEDOT:PSS-based Temperature Sensor with High Humidity Stability for Wireless Healthcare Monitoring," *Sc. Reports*, vol. 10, no. 1, pp. 2467, 2020.
- [40] M. Seifi, S. Hamedei, and Z. Kordrostami, "Fabrication of a high-sensitive wearable temperature sensor with an improved response time based on PEDOT:PSS/rGO on a flexible kapton substrate," *J. Materials Science: Materials in Electronics*, vol. 33, no. 9, pp. 6954-6968, 2022.
- [41] O. Ozioko, Y. Kumaresan, and R. Dahiya, "Carbon Nanotube/PEDOT: PSS Composite-based Flexible Temperature Sensor with Enhanced Response and Recovery Time," *IEEE Int. Conf. on Flexible and Printable Sensors and Systems (FLEPS)*, Manchester, UK, 2020, pp. 1-4, doi: 10.1109/FLEPS49123.2020.9239431.
- [42] X. Liao, Q. Liao, Z. Zhang, X. Yan, Q. Liang, Q. Wang, M. Li, and Y. Zhang, "A Highly Stretchable ZnO@Fiber-Based Multifunctional Nanosensor for Strain/Temperature/UV Detection," *Adv. Functional Materials*, vol. 26, no. 18, pp. 3074-3081, 2016.
- [43] C. Liu, S. Han, H. Xu, J. Wu, and C. Liu, "Multifunctional Highly Sensitive Multiscale Stretchable Strain Sensor Based on a Graphene/Glycerol-KCl Synergistic Conductive Network," *ACS Applied Materials & Interfaces*, vol. 10, no. 37, pp. 31716-31724, 2018.
- [44] A. Beniwal, P. Ganguly, D. K. Neethipathi, and R. Dahiya, "PEDOT:PSS modified Screen Printed Graphene-Carbon Ink based Flexible Humidity Sensor," *IEEE Int. Conf. on Flexible and Printable Sensors and Systems (FLEPS)*, Vienna, Austria, 2022, pp. 1-4, doi: 10.1109/FLEPS53764.2022.9781534.
- [45] Q. Zhao, Z. Yuan, Z. Duan, Y. Jiang, X. Li, Z. Li, and H. Tai, "An ingenious strategy for improving humidity sensing properties of multi-walled carbon nanotubes via poly-L-lysine modification," *Sensors and Actuators B: Chemical*, vol. 289, pp. 182-185, 2019.
- [46] J. Zhou, D. H. Anjum, L. Chen, X. Xu, I. A. Ventura, L. Jiang, and G. Lubineau, "The temperature-dependent microstructure of PEDOT/PSS films: insights from morphological, mechanical and electrical analyses," *Journal of Materials Chemistry C*, vol. 2, no. 46, pp. 9903-9910, 2014.
- [47] J. Neto, A. S. Dahiya, and R. Dahiya, "Influence of Encapsulation on the Performance of V₂O₅ Nanowires-Based Temperature Sensors," *IEEE Int. Conf. on Flexible and Printable Sensors and Systems (FLEPS)*, Vienna, Austria, 2022, pp. 1-4, doi: 10.1109/FLEPS53764.2022.9781483.
- [48] A. M. Nardes, M. Kemerink, and R. A. J. Janssen, "Anisotropic hopping conduction in spin-coated PEDOT:PSS thin films," *Physical Review B*, vol. 76, no. 8, pp. 085208, 2007.



Ajay Beniwal is currently working as a Marie Curie Early-Stage Researcher in Bendable Electronics and Sensing Technologies (BEST) Group, Electronics and Nanoscale Engineering, University of Glasgow, U.K. He received his PhD degree from the Department of Electronics and Communication Engineering, Indian Institute of Information Technology, Allahabad, Prayagraj, India in 2021. He completed his Bachelor's and Master's degree in Electronics and Communication Engineering from Kurukshetra University Kurukshetra, India, in 2013 and 2015, respectively. His current research interest includes material characterization and thin film technology, electronic sensor devices, printed and flexible electronics, for healthcare and agriculture applications. He holds the prestigious Marie Skłodowska-Curie Postdoctoral Fellowships (UKRI funded).



Deepan Kumar Neethipathi received his bachelor's degree in Chemical engineering (B.Tech) from Anna University, India in 2017, and later, his master's degree in Energy Science and Engineering (M.S) from Daegu Gyeongbuk Institute of Science and Technology, South Korea (DGIST) in 2020. Under the AQUASENSE project, he is working as a

Marie Curie Early-Stage researcher at Bendable Electronics and Sensing Technologies (BEST) group, Electronics and Nanoscale Engineering, University of Glasgow from October 2020. Currently, he is doing the second year of his Ph.D. studies in the Department of Geography and Earth science at the University of Glasgow, United Kingdom. His current research interest includes electrochemical sensors for water quality monitoring sensors and food quality-based application purposes.



Ravinder Dahiya (Fellow, IEEE) is Professor in ECE Department at Northeastern University, Boston, USA. He is the leader of Bendable Electronics and Sustainable Technologies (BEST) research group (formerly, Bendable Electronics and Sensing Technologies (BEST) group). His

> REPLACE THIS LINE WITH YOUR MANUSCRIPT ID NUMBER (DOUBLE-CLICK HERE TO EDIT) <

group conducts fundamental and applied research in flexible and printable electronics, tactile sensing, electronic skin, robotics, and wearable systems. He has authored or co-authored about 500 publications, books and submitted/granted patents and disclosures. He has led several international projects. He is President (2022-23) of the IEEE Sensors Council. He is the Founding Editor in Chief of IEEE JOURNAL ON FLEXIBLE ELECTRONICS (J-FLEX) and has served on the editorial boards of IEEE SENSORS JOURNAL (2012-2020) and IEEE TRANSACTIONS ON ROBOTICS (2012-2017). He was the Technical Program co-chair of IEEE Sensors 2017 and IEEE Sensors 2018 and has been General Chair/Co-Chair of several conferences including IEEE FLEPS (2019, 2020, 2021), which he founded in 2019, and IEEE Sensors 2023. He is recipient of EPSRC Fellowship, Marie Curie and Japanese Monbusho Fellowships. He has received several awards, including 2016 Microelectronic Engineering Young Investigator Award (Elsevier), 2016 Technical Achievement Award from the IEEE Sensors Council and 12 best paper awards as author/co-author in International Conferences and Journal.